Chapter 2

Accelerometer Theory & Design

2.1 Introduction

An accelerometer is a sensor that measures the physical acceleration experienced by an object due to inertial forces or due to mechanical excitation. In aerospace applications accelerometers are used along with gyroscopes for navigation guidance and flight control. Conceptually, an accelerometer behaves as a damped mass on a spring. When the accelerometer experiences acceleration, the mass is displaced and the displacement is then measured to give the acceleration [17].

In these devices, piezoelectric, piezoresistive and capacitive techniques are commonly used to convert the mechanical motion into an electrical signal. Piezoelectric accelerometers rely on piezoceramics (e.g. lead zirconate titanate) or single crystals (e.g. quartz, tourmaline). They are unmatched in terms of their upper frequency range, low packaged weight and high temperature range. Piezoresistive accelerometers are preferred in high shock applications. Capacitive accelerometers performance is superior in low frequency range and they can be operated in servo mode to achieve high stability and linearity.

Modern accelerometers are often small micro electro-mechanical systems (MEMS), consisting of little more than a cantilever beam with a proof-mass (also known as seismic-mass) realized in single crystal silicon using surface micromachining or bulk micromachining processes.

2.2 Working principle of accelerometer

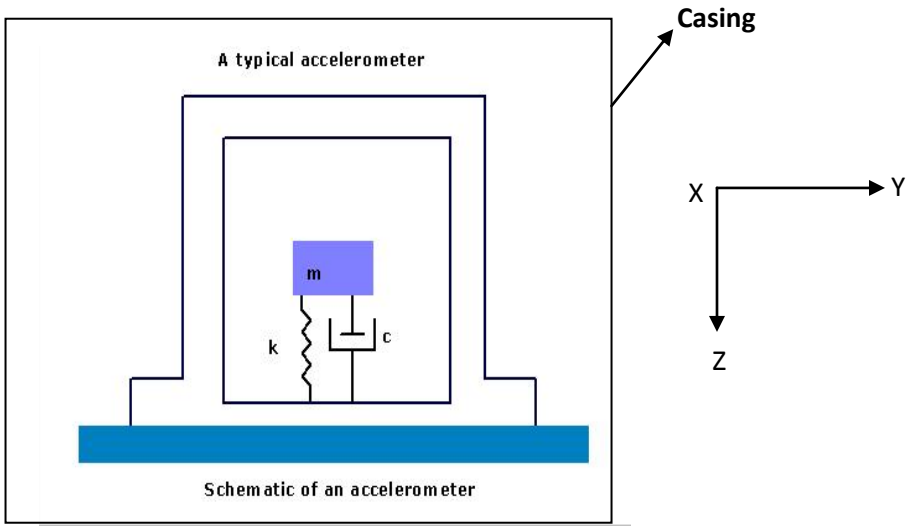

Fig. 2.1 Schematic of an accelerometer

The principle of working of an accelerometer can be explained by a simple mass (m) attached to a spring of stiffness (k) that in turn is attached to a casing, as illustrated in fig 2.1. The mass used in accelerometers is often called the seismic-mass or proof-mass. In most cases the system also includes a dashpot to provide a desirable damping effect.

The dashpot with damping coefficient (c) is normally attached to the mass in parallel with the spring. When the spring mass system is subjected to linear acceleration, a force equal to mass times acceleration acts on the proof-mass, causing it to deflect. This deflection is sensed by a suitable means and converted into an equivalent electrical signal. Some form of damping is required, otherwise the system would not stabilize quickly under applied acceleration.

To derive the motion equation of the system Newton's second law is used, where all real forces acting on the proof-mass are equal to the inertia force on the proof-mass. Accordingly a dynamic problem can be treated as a problem of static equilibrium and the equation of motion can be obtained by direct formulation of the equations of equilibrium. This damped mass-spring system with applied force constitutes a classical second order mechanical system.

From the stationary observer's point of view, the sum of all forces in the z direction is,

$$F_{applied} - F_{damping} - F_{spring} = m\ddot{x}$$

$$m\ddot{x} + F_{damping} + F_{spring} = F_{applied}$$

$$m\ddot{x} + kx + \dot{c}x = F \quad (2.1)$$

Where

m = mass of the proof-mass

x = relative movement of the proof-mass with respect to frame

c = damping coefficient

k = spring constant

F = force applied

The equation of motion is a second order linear differential equation with constant coefficients. The general solution x (t) is the sum of the complementary function X_C (t) and the particular integral Xp (t) [18].

$$X = X_C(t) + X_P(t) \quad (2.2)$$

The complementary function satisfies the homogeneous equation

$$m\ddot{x} + kx + c\dot{x} = 0 \quad (2.3)$$

The solution to $X_C(t)$ is

$$X_C(t) = Ce^{st} \quad (2.4)$$

Substituting (2.4) in (2.3)

$(ms^2 + cs + k)\ C\ e^{st} = 0$

As Ce^{st} cannot be zero for all values of t, then $(ms^2 + cs + k) = 0$ called as the auxiliary or characteristic equation of the system. The solution to this equation for values of S is

$$S_{1,2} = \frac{1}{2}m(-C \pm \sqrt{C^2 - 4mk}) \quad (2.5)$$

From the above equation 2.5, the following useful formulae are derived

$$\omega_n = \sqrt{\frac{k}{m}} \quad (2.6)$$

$$c/m = 2\ \zeta\ \omega_n \quad (2.7)$$

$$\zeta = c/2\ \sqrt{km} \quad (2.8)$$

Where

ω_n = undamped resonance frequency

k = spring constant

m = mass of proof-mass

c = damping coefficient

ζ = damping factor

Steady state performance

In the steady state condition, that is, with excitation acceleration amplitude 'a' and frequency 'ω', the amplitude of the response is constant and is a function of excitation amplitude and frequency 'ω'. Thus for static response 'ω'=0, the deflection amplitude

$X = X_0 = F/k.$

$$X = ma / k \tag{2.9}$$

Here the sensitivity 'S' of an accelerometer is defined by,

$$S = X / a = m/k \tag{2.10}$$

Dynamic performance

For the dynamic performance it is easier to consider the Laplace transform of eqn (2.1)

$$\frac{x(s)}{a(s)} = \frac{1}{s^2 + \frac{c}{m}s + \frac{k}{m}} \tag{2.11}$$

It can be seen by comparing eqn (2.6) and (2.10) that the bandwidth of an accelerometer sensing element has to be traded off with its sensitivity since $S \alpha 1/\omega_n^2$ (this trade off can be partly overcome by applying feedback , i.e closed loop scheme).

The sensor response is determined by damping present in the system. A damping factor (ζ) between 0.6 to 1.2 results in high response time, fast settling time, good bandwidth and linearity.

2.3 Specifications of the accelerometer

The accelerometer that is to be designed shall have a measuring range of ±30 'g' with a resolution of 50 milli 'g' i.e a dynamic range of 600. The total non-linearity from the sensor element, electronics and from other sources shall not be more than 1% of full scale output (FSO). The sensor shall have a bandwidth (± 3dB) of >100 Hz and the cross-axis sensitivity shall be limited to a maximum of 1% of FSO. The sensor's bias stability and hysteresis values are specified as 0.15% of FSO each. Finally the sensor shall have a response time of less than 1msec and it shall perform over a temperature range of -20 to 80°C.

2.4 Configuration of accelerometer

Various aspects are taken in to consideration before finalizing the configuration of the accelerometer. Special attention is paid to the available fabrication processes, signal conditioning electronic circuit, material selection, electrical routing and packaging. The configuration of the accelerometer is as shown in fig 2.2.

(i) The sensor is configured to have a three wafer (glass-silicon-glass) configuration.

(ii) Differential capacitance transduction method is selected as it offers the advantages of low temperature sensitivity, higher transduction

efficiency and the method can be readily adopted for closed loop operation.

(iii) Glass wafers are used for the top and bottom plates and a thin film of aluminum material is deposited on the inner side of glass wafers using E-beam metal evaporation process. The central wafer consists of the active proof-mass which moves as a function of the applied acceleration thereby causing change in capacitance.

(iv) The proof-mass is supported on all four sides by L-shaped beams. The proof-mass exhibits piston like movement and remain parallel to electrodes at all accelerations. Also any geometrical change in the beam length due to temperature variation, limits the proof-mass to in-plane rotation only and it does not experience any out of plane bending. This configuration reduces the overall sensor chip size thereby improving the per wafer yield and also reduces the non-linearity associated with cantilever type support structures.

(v) The mechanical support for the proof-mass is provided at the central plane of the proof-mass. Positioning of the beams at central plane of proof-mass will reduce the cross-axis sensitivity of the sensor.

(vi) The proof-mass to electrode gap is selected as 22 microns, this eliminates the requirement of complicated device level vacuum

sealing and also need for perforations on the proof-mass thus simplifying the process.

(vii) Bulk micro-machining process using KoH is considered for realizing the micro structures.

(viii) Modular concept is used for realizing the final device. MEMS chip and the signal conditioning electronics are realized separately and packaged on a signal platform.

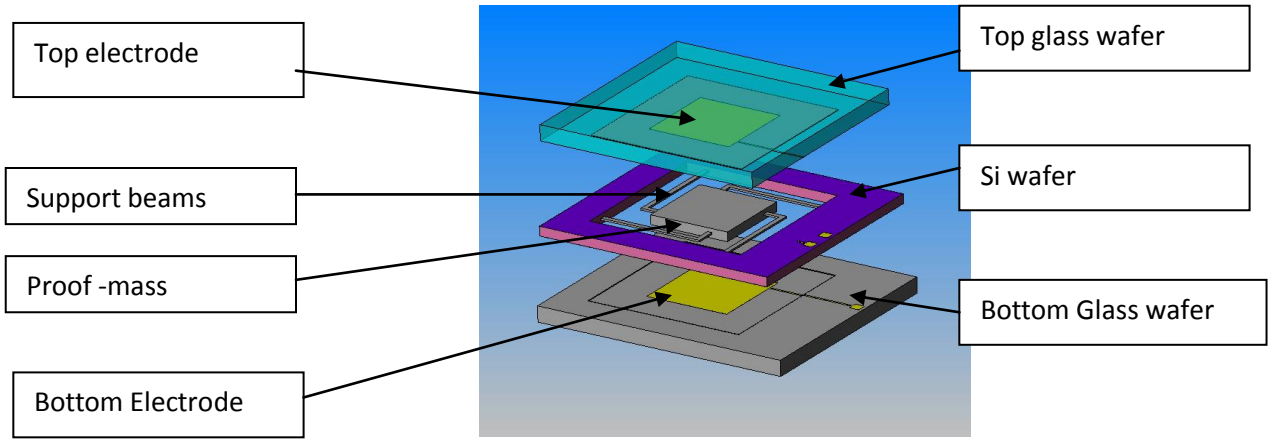

Fig 2.2 Accelerometer configuration

2.5 Material selection

Single crystal silicon (100) material is selected for accelerometer structure. Silicon is almost an ideal structural material, it has about the same young's modulus as steel but is as light as aluminum. The melting point of silicon is 1400^0 C and the thermal expansion coefficient is much

less than steel which makes it dimensionally stable even at high temperatures. Silicon wafers are extremely flat, can accept coatings & additional thin-film layers for building microstructures. Silicon exhibits no mechanical hysteresis and precise geometrical features can be realized using standard photolithography and etching techniques. Electrically conductive silicon with resistivity 0.1 Ω-cm is selected for the proof-mass. Similarly Pyrex 7740 glass is chosen for top and bottom wafers to reduce stray capacitance and to provide required sealing. The glass wafers are bonded to silicon wafer using anodic bonding process. Electrodes and electrical contact pads are realized by depositing sub-micron thickness Aluminum coating, using E-beam evaporation process. The material properties of silicon and Pyrex glass are shown in Table 2.1

Material Property	**Silicon**	**Pyrex glass**
σ_y (yield strength) 10^9 N/m^2	7	0.5-0.7
E (Young's modulus)10^{11}N/m^2	1.69	400
ν (Poisson's ratio)	0.28	0.17
α (thermal expansion coefficient)10^{-6} mt/mt° C	2.5	0.5
ρ (density) g/cm^3	2.3	2.225

Table 2.1: Material properties of silicon and Pyrex glass.

2.6 Analytical design

The following assumptions are made to begin the design work

(i) The proof-mass size and spring stiffness are selected in such a way that there shall be a capacitance change of around 1fF for 50 milli 'g' (minimum resolution). This limitation comes from the capacitance signal that can be handled comfortably by the electronics scheme.

(ii) For calculating the proof-mass to electrode gap and damping aspects, the micro structure is considered as working under ambient pressure conditions. This is due to fabrication facility limitation in chip level sealing under vacuum.

The structural parameters of the proof-mass are optimized to achieve the required sensitivity and bandwidth. The proof-mass length, width, thickness are represented as l_1, b_1, h_1. The L- Beam dimensions are represented by l_2, l_3, b_2, and h_2 respectively, which are shown in fig.2.3.

The optimized device dimension are given below

Proof-mass size (l_1 X b_1 X h_1)	:	2500 X 2500X 300 μm
Length of beam (l_2)	:	3200 μm
Length of beam (l_3)	:	640 μm

Beam Width (b_2) : 150 µm

Beam thickness (h_2) : 55 µm

Air gap : 22 µm

(i) Area of the proof-mass (A) = l_1 X b_1 = 6.25 x10^{-6} m^2

(ii) Mass of proof-mass (m) = $V.\ \rho$ = (A x $h1$) x ρ = 4.313 x10^{-6} Kg

(Density of the silicon ρ = 2300 kg/m^3, V = Volume of proof-mass)

Mass of the beams (m_b) = 4(l_2+l_3) x b_2 x h_2 x ρ = 2.91456 x10^{-7} Kg.

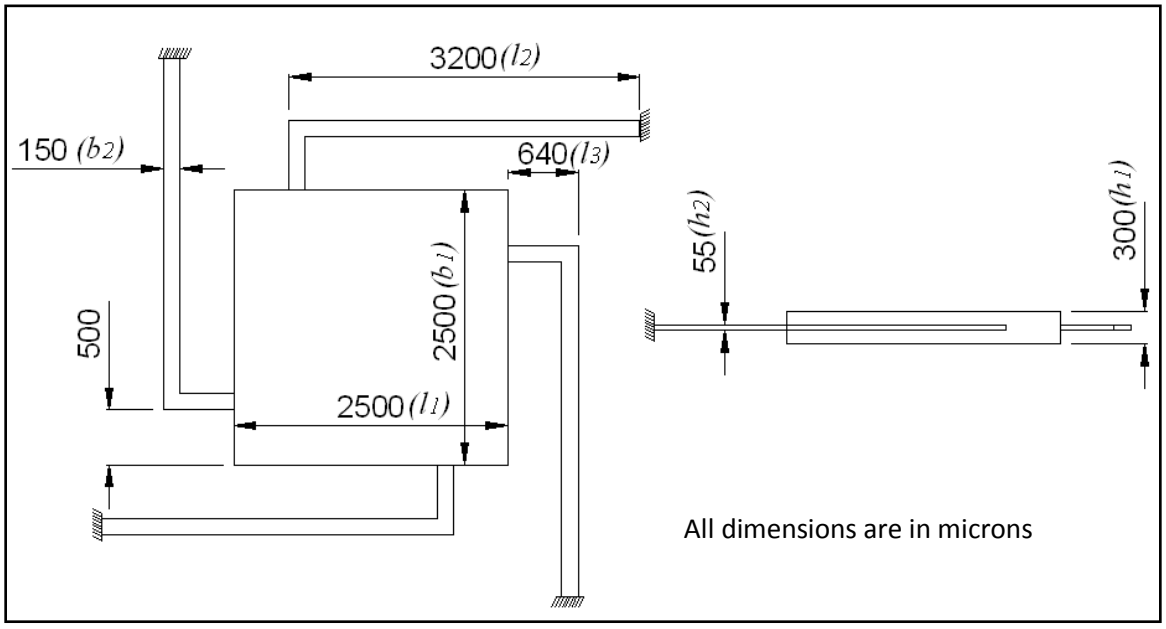

Fig 2.3 Accelerometer geometrical details

(iii) Maximum force on the proof-mass

Let 'F' be the force acting on the proof-mass, due to 1 g acceleration, which is given by the relation.

F = m x a

Where 'm' is the mass of the proof-mass and 'a' is the acceleration

F = 4.313 e-6 X 9. 81 X 1 = 0.0423 mN

This force is shared by all the beams equally.

Force acting on each beam W = F/4 = 0.01057mN

(vi) Moment of inertia of beams

$$I = \left(\frac{b_2 h_2^3}{12}\right) = \quad 2.07 \text{ e-18} \quad m^4$$

(v) Deflection of the beam

The L beam is rigidly fixed to the frame on one side and other side is attached to the Proof-mass. This can be considered as two cantilever springs in series, rigidly fixed on one side and guided on the other side. The numerical equation for the above is given as

$$\text{Deflection } \delta = \frac{Wl^3}{12EI}$$

Where E = Modulus of elasticity for silicon E=1.69 x 10^{11} N/m^2

I= moment of inertia of beam.

For beam having length l_2 $\delta 1 = \frac{Wl_2^3}{12EI}$

For beam having length l_3 $\delta 2 = \frac{Wl_3^3}{12EI}$

$\delta = \delta 1 + \delta 2 = \frac{W\left(l_1^3 + l_2^3\right)}{12EI}$

$\delta = 8.3166 \times 10^{-8} m/g$

At 30g the maximum deflection =2.49 x10^{-6} m

(vi) Bending stress in the beam

The formula for determining the bending stress in a beam under simple bending is given by

$$\sigma_b = \frac{M}{I} \times y$$

Where

σ_b = Bending stress in the beam

M = Bending moment acting on the beam

y = the perpendicular distance to the neutral axis.

At 30 g

$$M = W \times l_2 \times 30$$
$$M = 0.01057 \times 10^{-3} \times 3200 \times 10^{-6} \times 30$$
$$M = 1.014 \times 10^{-6} Nm$$

For maximum bending stress $y = h_2/2$

$$\sigma = 13.4 MPa$$

(vii) Factor of safety

Since silicon is a brittle material, the UTS value is taken for calculating the factor of safety design margin over the theoretical design capacity.

Calculating factor of safety at 30g

FOS = ultimate strength / maximum stress

= 7000 / 13.4 = 522

(viii) Natural frequency

The natural frequency f_n of the spring mass system is given by

$$f_n = \frac{1}{2\Pi}\sqrt{k/m} \qquad (2.12)$$

Where 'k' is the stiffness of the spring

$$k = \frac{F}{\delta} = 508.62 \text{ N/m}$$

From equation 2.12 f_n = 1728Hz.

2.7 Electrical design

Capacitance is the ability of a body to hold an electric charge. The capacitance between two parallel plate conductors can be calculated if the geometry of the conductor and the dielectric properties of the insulator between the conductors are known.

(i) Nominal Capacitance (C_o)

The Nominal Capacitance of a parallel plate capacitor with overlapping area `a' separated by a distance `d' is equal to

$$C_o = \frac{\in_r \in_0 a}{d} \tag{2.13}$$

Where

$\in_r$ = Relative permittivity of the dielectric medium (for Air $\in_r$ =1)

$\in_0$ = Permittivity of free space = 8.85 x 10^{-12} F/m

C_o= 2.514 pF

(ii) Accelerometer Sensitivity

The initial gap between the proof-mass and the electrode is 22μm. Let C_1 and C_2 are capacitances between top electrode and proof-mass and bottom electrode and proof-mass respectively under the application of 1 'g'. Since the system is a differential capacitor, under the influence of gravitation force, as one side capacitance increases the other side it decreases.

$$C_1 = \frac{\in_0 \in_r a}{d + \partial}$$
$$C_1 = 2.5047\,pF$$
$$C_2 = \frac{\in_0 \in_r a}{d - \partial}$$
$$C_2 = 2.5237\,pF$$

Change in capacitance is therefore calculated as,

$$\Delta C = C2 - C1 \qquad (2.14)$$
$$= 19\ fF$$

Sensitivity = ΔC / applied acceleration

$$= 19\ fF/g$$

2.8 FEM modelling and simulation

The design and development of a MEMS device is highly challenging task involving simulation of micro structure behavior under coupled environmental load conditions. FEM is an essential tool for MEMS design and it provides accurate stimulation of the static and dynamic behavior of complex structures at micro scale. Several FEM tools are available in the mrket for MEMS modelling and simulation. However in this case, Coventorware software is used for accelerometer modelling and FEM analysis, Intellisuite software is used for wet etching process simulation and SABER for system level simulation.

In Coventorware solid models are built from 2-D layout tool with process information and meshes are created on solid models in the

preprocessor. Coventorware analyzer module uses various numerical approaches such as 3-D FEM of MEMMECH, 3-D BEM of MEMELECTRO modules for solving the partial differential equations of mathematical physics.

Since our accelerometer structure has regular shaped beams and plates, an eight node manhattan brick element is used for meshing the model. The element has an orthogonal geometry i.e all model faces are planar and join at right angles. The model is meshed with uniform mesh density through the model to reduce errors.

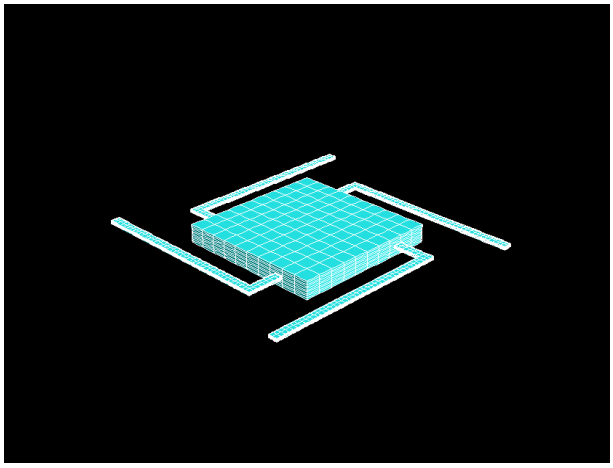

Fig 2.4 Meshed model of accelerometer structure

2.9 Mesh convergence study

The accuracy of a discrete solution of a partial differential equation depends on the density of the mesh. Therefore, the accuracy of an analysis can only be judged by the comparison of results on meshes of increasing degrees of freedom i.e. studying mesh convergence. To study

mesh convergence multiple mesh models of different densities are created. The mesh density on the beams is gradually increased by reducing the element size while keeping the aspect ratio same. The proof-mass is meshed with a mesh density of 600 throughout the study. The results of the proof-mass displacement (microns) with 1 'g' acceleration as a function of mesh density of the beams are plotted in fig 2.5.

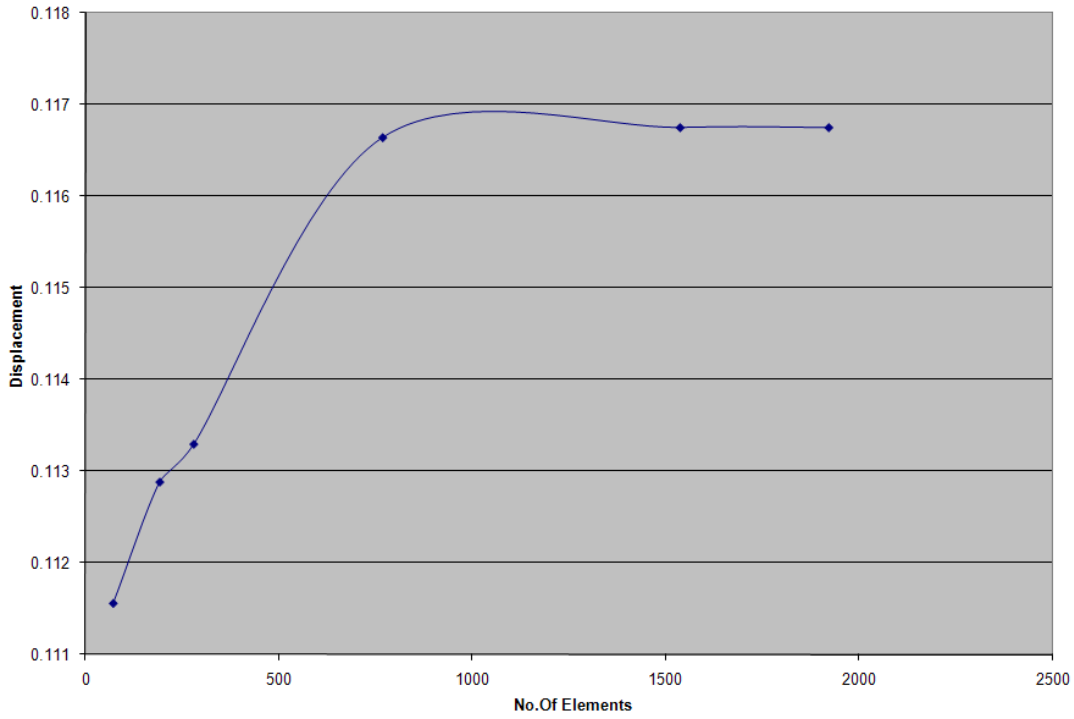

Fig 2.5 Mesh convergence simulation result

From fig 2.5, it can be seen that for a mesh density of 800 elements and more on the beams, the change in variation of proof-mass displacement is less than 1%, hence convergence is achieved. All further analysis is done considering the optimized mesh density. Elements on the L-beam

joining face to the frame are completely constrained and all other elements have 6 degrees of freedom.

2.10 FEM simulation results

The model is subjected to acceleration load upto 30 'g' and the response of the sensor for displacement, change in capacitance, bending stresses and cross-axis sensitivity are studied.

2.10.1 Acceleration vs. displacement

The structure is subjected to 0 'g' to 30 'g' acceleration in +Z direction, in steps of 3 'g' to analyze the proof-mass displacement. The analysis results are shown in table 2.2. The maximum displacement of the proof-mass in Z-direction is 3.48 microns.

Acceleration (g)	0	3	6	9	12	15	18	21	24	27	30
Displacement (μm)	0	0.348	0.696	1.044	1.392	1.74	2.088	2.436	2.784	3.132	3.48

Table 2.2 Acceleration Vs displacement of proof-mass

As shown in table 2.2 & fig 2.6, the proof-mass displacement is linear with respect to the applied acceleration.

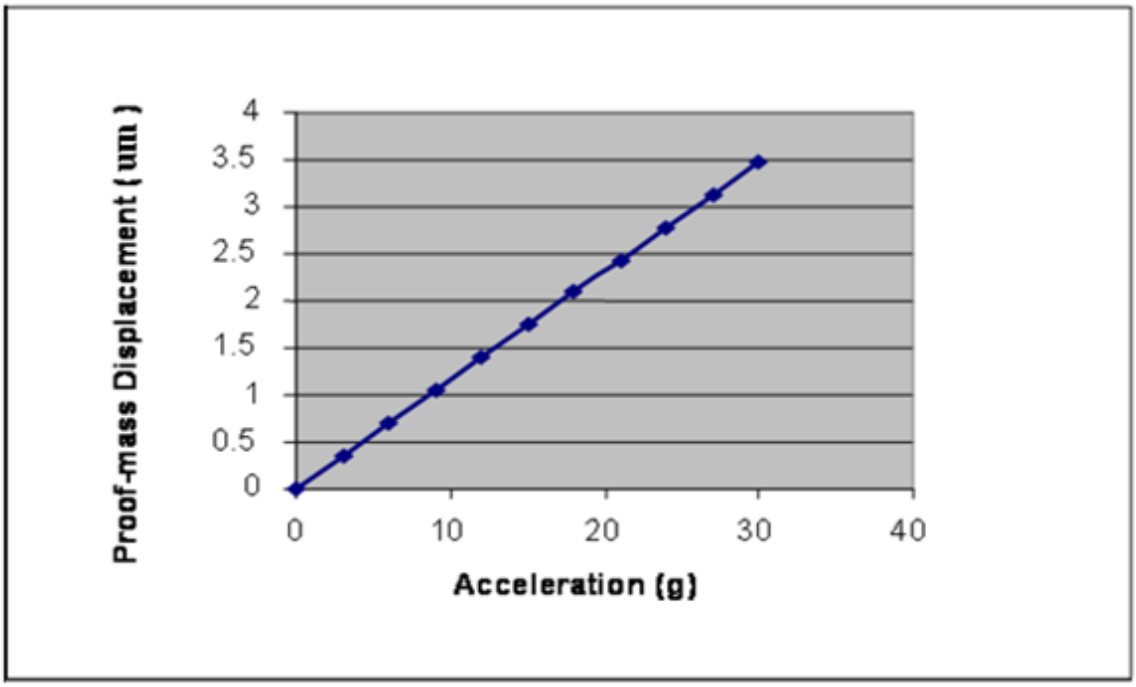

Fig 2.6 Applied acceleration Vs Proof- mass displacement

2.10.2 Acceleration vs. capacitance

Coupled electro-mechanical simulation is done for the accelerometer by applying a voltage of 5V on the top and bottom electrodes and grounding the proof-mass. The accelerometer is subjected to acceleration varying from 0 'g' to 30 'g' in both + Z and – **Z** direction. The capacitances across top electrode and proof-mass, bottom electrode and proof-mass are obtained. The nominal capacitance of the accelerometer is 2.514 pF. The resultant change in capacitance value in steps of 3 'g' is given in Table 2.3 and the sensitivity of the accelerometer is 27.4 fF/g.

ACCELERATION (g)	CHANGE IN CAP. FOR POSITIVE ACC. (pF)	CHANGE IN CAP. FOR NEGATIVE ACC. (pF)
0	0	0
3	0.080249	-0.08011
6	0.16055	-0.16041
9	0.24119	-0.24095
12	0.321998	-0.32185
15	0.403377	-0.40324
18	0.485374	-0.48524
21	0.568108	-0.56797
24	0.651715	-0.65158
27	0.73633	-0.73619
30	0.822097	-0.82196

Table 2.3 Acceleration Vs change in capacitance

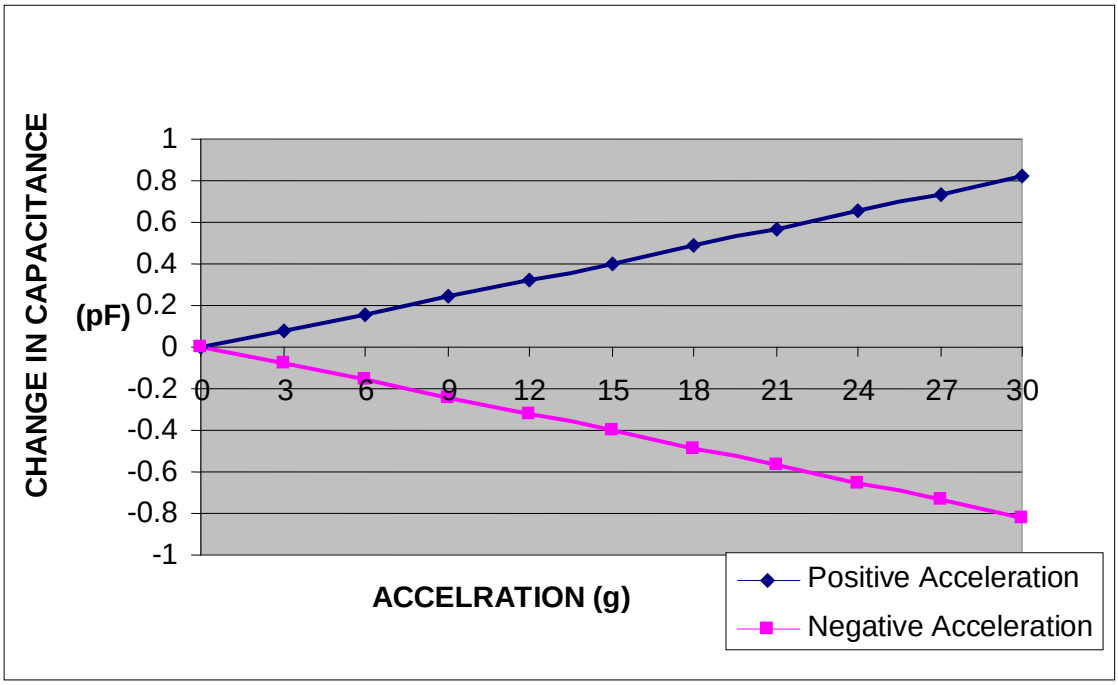

Fig 2.7 Change in capacitance with acceleration

From the change in capacitance equation 2.14, it can be seen that the change in capacitance is non–linear with applied acceleration. The above data is analyzed for non-linearity using least square method curve fitting technique. The equation of the best fit line is y = 27.3684x + (-3.5698) and the maximum non-linearity is 0.764% which is well within the design requirement.

2.10.3 Bending stresses in the beams

Maximum bending stress occurs in L-beams due to the applied acceleration in the Z direction. The maximum bending stress is occurring at the point where the L-beam is anchored to the frame and at the sharp corner of the L beam, fig 2.8 gives the stress distribution in the model. The magnitude of maximum von Mises stress at 30 ‘g’ acceleration is 11 MPa, which is much less than the UTS value of silicon which is 7000 MPa.

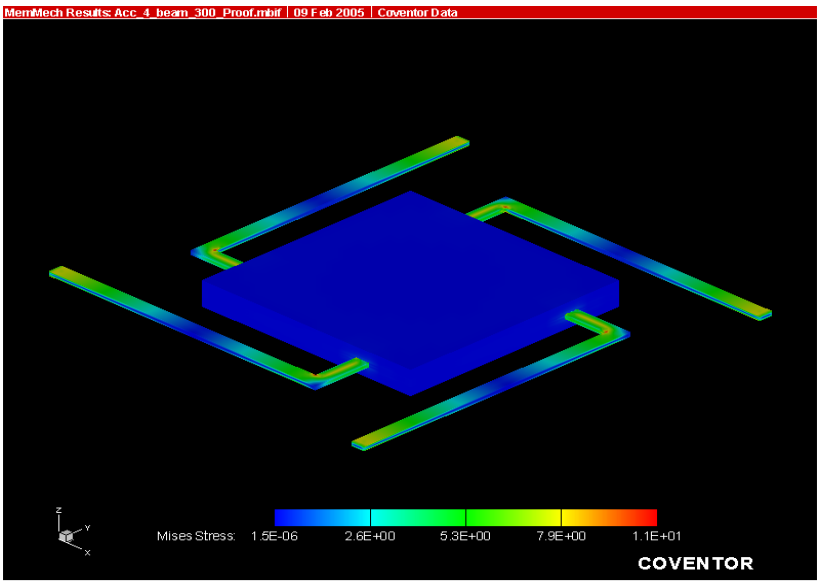

Fig 2.8 Stress distribution in the accelerometer at 30 ‘g’

2.10.4 Modal analysis

Modal analysis is done to obtain the first and second mode frequencies of the accelerometer. The first mode resonant frequency of the structure is, out of plane vibration along Z axis which is at 1470 Hz. The thumb rule is that the first mode resonant frequency of the structure shall be at least three times the required bandwidth. The second mode frequency is, in X-Y plane at 3323 Hz. fig. 2.9 shows the modes of vibration. Both the frequency modes of operation are far away from the maximum operational bandwidth of 100Hz, hence no interference on accelerometer functioning is expected.

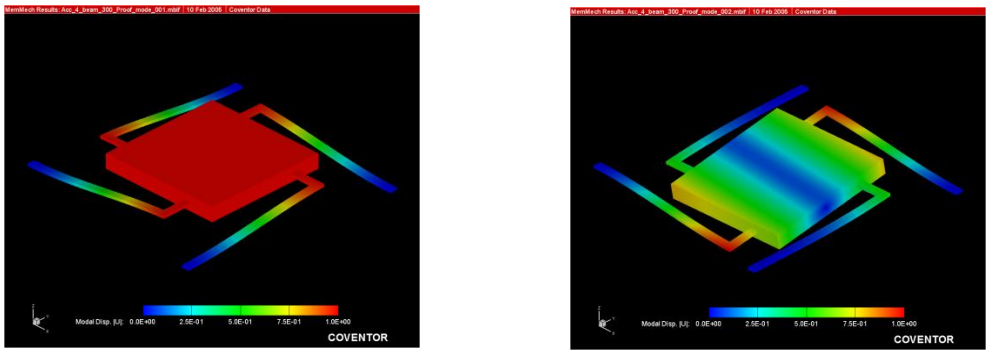

Mode 1:1470Hz **Mode 2: 3323Hz**

Fig 2.9 Modal analysis results of the accelerometer structure

2.11 Cross - axis sensitivity

The accelerometer shall sense acceleration along the Z-axis only and it shall be insensitive to the applied acceleration along other two axes. The cross-axis sensitivity specification of the accelerometer is < 1% of FSO. As already presented earlier the proof-mass thickness is 300 μm and the supporting L-beam thickness is 55 μm. From fabrication process point of view, it is very easy to realize the beams aligned to the top or bottom plane of the proof-mass by etching the beams to the required thickness from one side. The accelerometer is symmetrical about x and y axes. The meshed accelerometer model is subjected to cross acceleration along X-axis for three different beam positions along the thickness of the Proof-mass.

The results are shown in fig 2.10. The cross-axis sensitivity increases as function of the distance from central plane of the proof-mass. For the beam position, at the central plane of the proof-mass, the cross-axis sensitivity obtained is 0.01% of FSO, hence the position of the support beams is finalized at the center of the proof-mass.

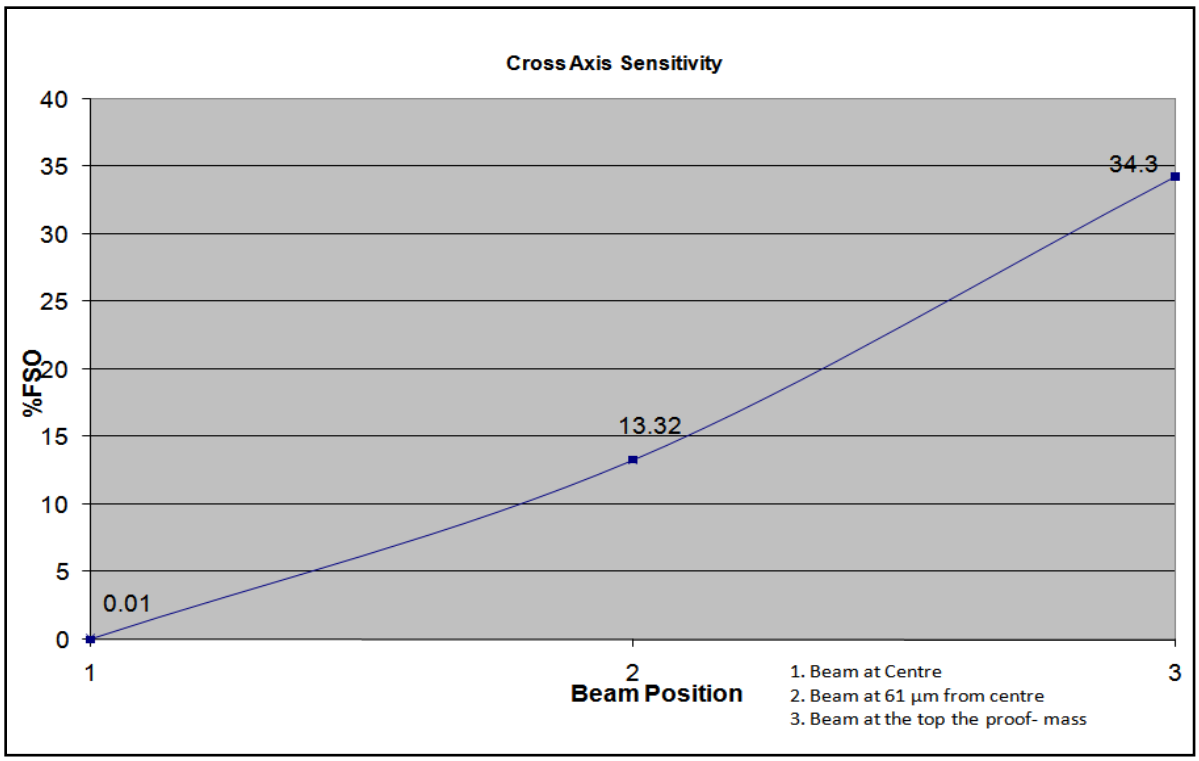

Fig 2.10 Effect of beam position on the cross axis sensitivity

2.12 System level simulation of the sensor

Traditionally MEMS devices have been simulated using field solvers, such as finite element method (FEM) and boundary-element method (BEM) analysis tools. These tools solve complex partial differential equations derived from the detailed description of the physical design, but those equations are far from simple and take a lot of time to solve.

However, in system level or high-level simulation method, simulations are done based on the behavior of a device as expressed by reduced-order equations [19]. It simulates the overall behavior of complete model instead of the interactive behavior of many finite elements that comprise the model. The complex mathematical description used with high-level models leads to a much smaller number of degrees of freedom that reduces the number of computations performed by the solver, resulting in much faster simulation runs. The higher level of abstraction and the physical analogy between translation, rotation, electronics, thermodynamics, and other entities permits the interconnection of a number of physical domains.

The system level simulation tool offered by Coventorware architect module called SABER is used in the present design. SABER uses behavioral model libraries. The models include underlying code that expresses the behavior of the individual components subjected to electrical, mechanical or other domain stimuli.

2.12.1 System level modelling

The system level accelerometer model (fig 2.11) is built using standard library components and consists of four support beam elements and a rectangular proof-mass plate. Two electrode elements at the top and bottom of the proof-mass allow electrostatic excitation and capacitive detection due to vibration.

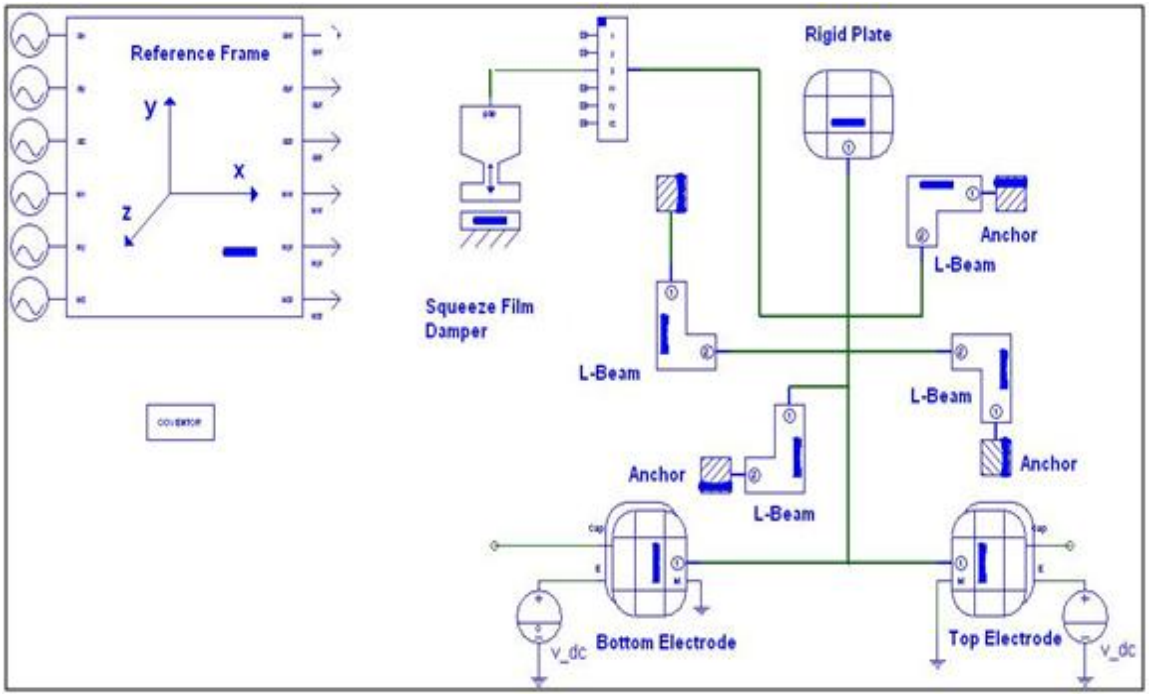

Fig.2.11 System level behavior model of the accelerometer

2.12.2 Small signal AC analysis

To determine the resonant behavior of the accelerometer structure a small signal AC analysis is performed. The model is excited over a frequency range of 1 Hz to 10 kHz. Fig 2.12 shows the maximum response and phase angle details as a function of the applied acceleration. It can be seen that the natural frequency of the system is 1432 Hz where the phase angle is 90 deg.

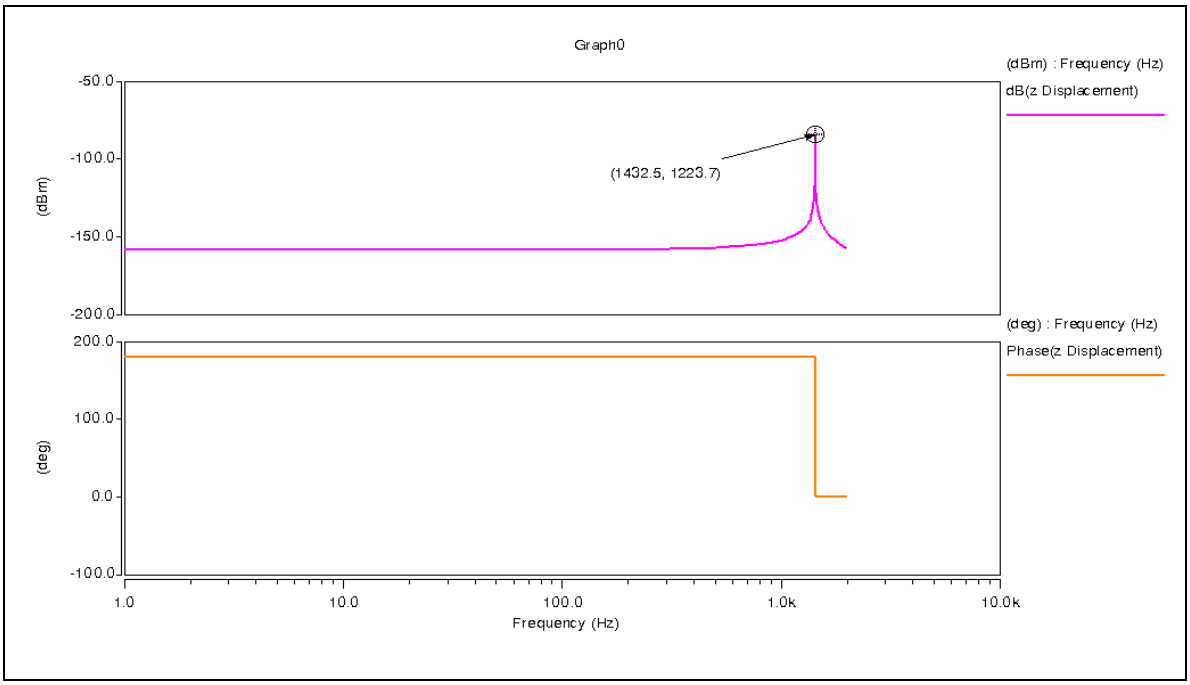

Fig 2.12 Small signal AC analysis results

2.12.3 Pull in analysis

During anodic bonding process of accelerometer, for bonding silicon wafers with glass wafers, upto 1000 VDC is applied between the wafers. At such high voltages due to electrostatic attraction the proof-mass may come in complete area contact with electrodes on the glass wafers and may not revert back to normal position due to stiction arising out of large area of contact. Pull in analysis is done to know the safe working voltage that can be applied between the proof-mass and electrodes. The analysis is done by grounding the proof-mass and varying bottom electrode voltage from 25 to 160 VDC.

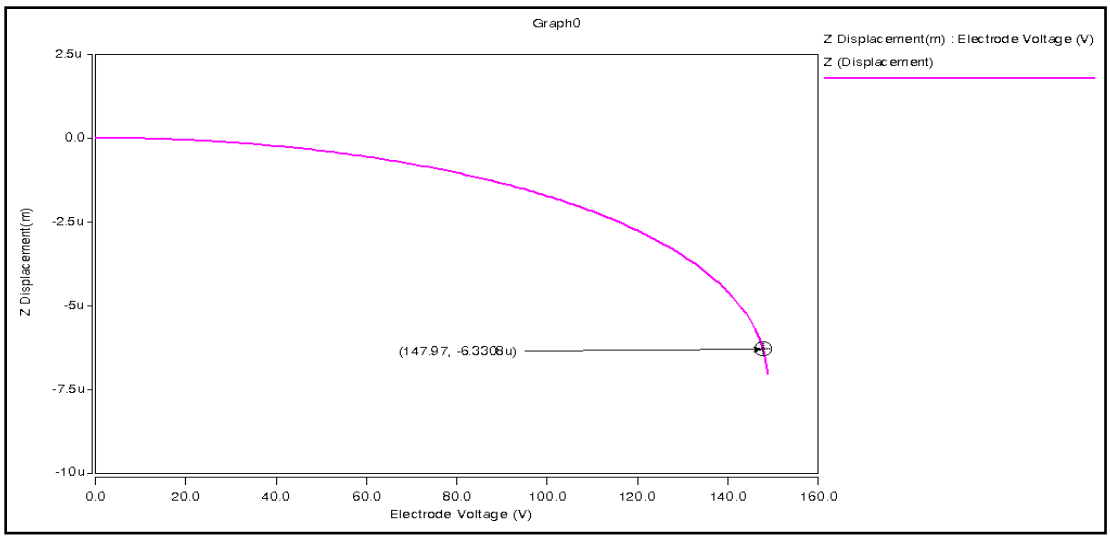

Fig 2.13 Pull in analysis result

As shown in fig 2.13 pull in analysis result, the electrostatic force overcomes spring force of the structure at pull in voltage of 147.97 V. Hence during fabrication suitable bumps are provided on the proof-mass to overcome stiction problem.

2.12.4 Transient analysis

Transient analysis is done to estimate the device sensitivity and response time to the applied acceleration input. The aerospace sensors need to have quick response and fast settling times. An acceleration of 1 'g' is applied on the structure in 0.1 micro-sec and withdrawn after 1m-sec in 1micro-sec. Fig 2.14 shows the result of transient analysis. The result shows that the displacement and capacitance change are very closely following the input 1 'g' signal. The system has response time of

less than 1 m-sec which is well within the design requirements of 1m-sec.

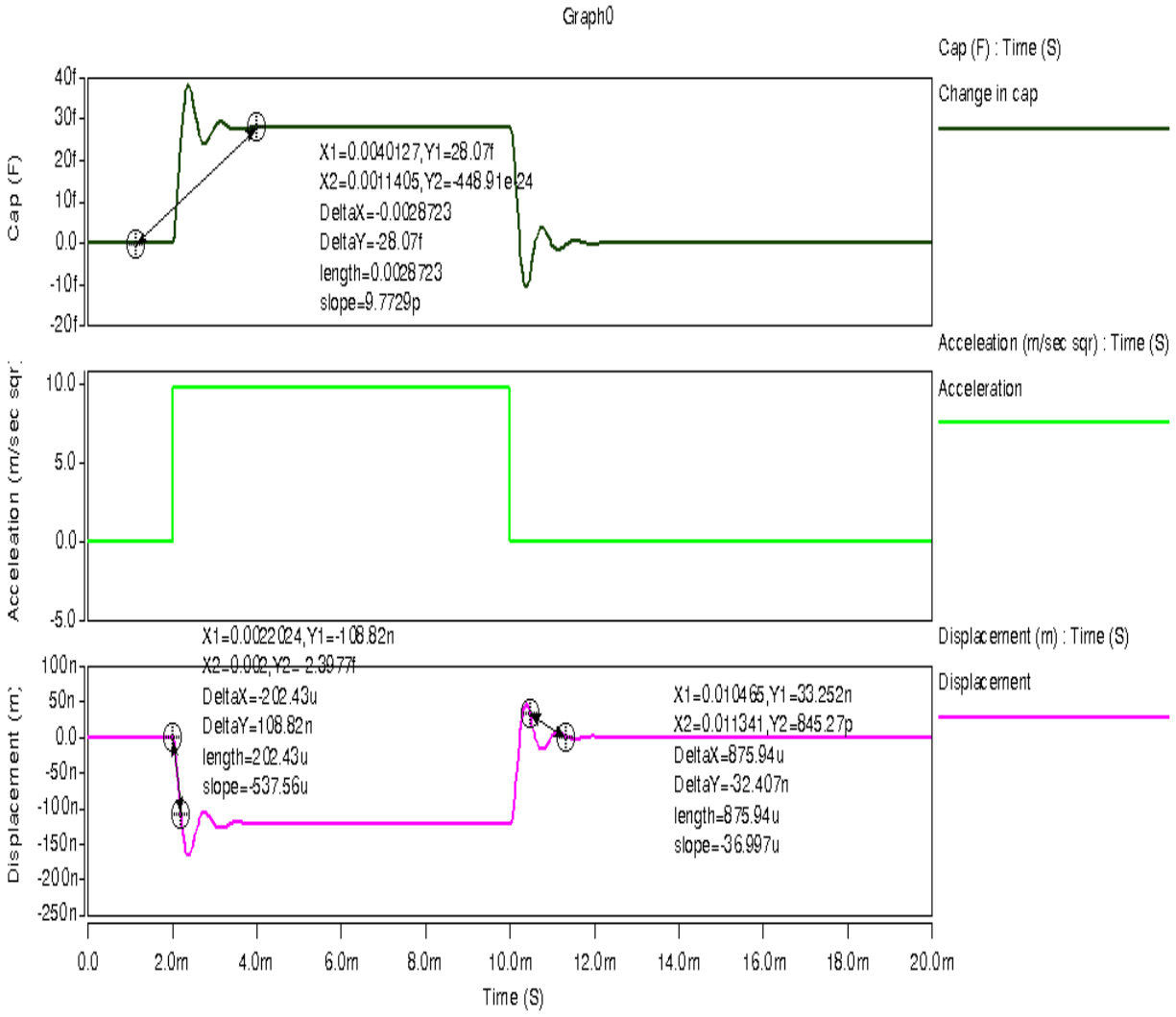

Fig 2.14 Transient analysis result with 1 'g' input signal

2.13 Dynamic analysis

In the current accelerometer design the sensing proof-mass is capped on both sides using glass wafers at atmospheric pressure. As the proof-mass moves towards the stationary electrodes, pressure between

the two layers increases developing damping forces. This pressure drives out the entrapped air between the parallel plates. On the contrary, when the proof-mass is moving away from the electrode the pressure in the gap is reduced causing surrounding air to flow into the gap. In both cases the force on the proof-mass caused by built-up pressure is always against the movement of the plate. The work done by the plate is consumed by the viscous flow of the air and transformed into heat. In other words, the air film acts as a damper and this type of damping is called squeeze film damping. The damping phenomenon is shown in fig.2.15. In the past, considerable research was done in characterizing squeeze film damping behavior in MEMS structures [20-29]. Veijola et al developed equivalent circuit model of squeeze film damping applicable to MEMS accelerometers using R-L elements [23]. Sadd et al considered the incompressible effects of gas at low squeeze numbers [27].

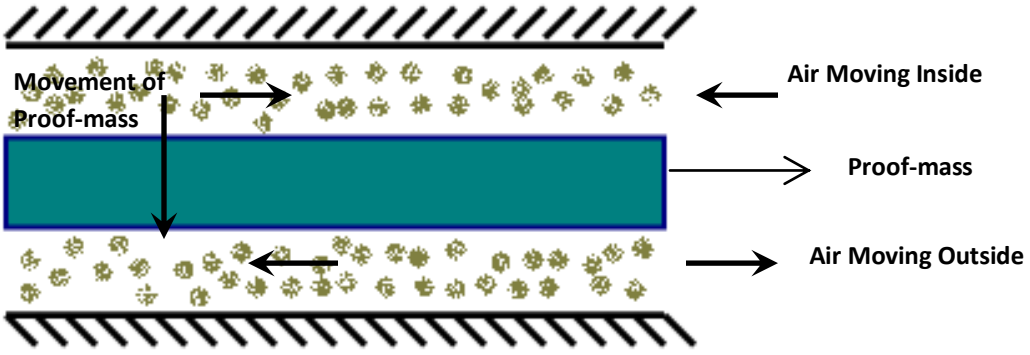

Fig.2.15 Damping phenomenon

2.13.1 Squeeze film damping

Starr proposed the following conditions which are to be satisfied to obtain satisfactory behavior of damping in micro accelerometers, [20].

1. The behavior of squeeze film is governed by both viscous and inertial effects. For small geometries inertial effects are neglected. The specific condition of validity is:

$$\omega d^2 \rho / \mu << 1.0 \tag{2.15}$$

Where

ω = frequency of oscillation of proof-mass

d = air gap

ρ = density of air 1.16 e^{-18} kg /m^3

μ = dynamic viscosity of the damping media i.e. air 1.86 x 10^{-11}N-sec/m

$$\frac{1470 \times 2\pi \times 22^2 \times 1.16 \times 10^{-18}}{1.86 \times 10^{-11}} = 0.2$$

2. The air flow is assumed as continuum, slip flow condition at the boundaries may reduce the effectiveness of damping.

To overcome this problem the film thickness shall be > (100 times mean free path of air) [20] [29]. At room temperature, the mean free

path of air is 0.065 microns. Hence, the film thickness shall be > 6.5 microns.

3. Squeeze no. σ which is dimensionless number, is a measure of compression of fluid in the gap. If σ is low (close to zero implying low speed), the gas film follows nearly incompressible viscous flow. If σ

is large (σ > 0.3), the film essentially acts as an incompressible

air spring and exhibits little energy dissipation.

$$\sigma = \frac{12\mu\omega b^2}{h_0^2 P_a} = 0.26 \qquad (2.16)$$

Where ω = frequency of oscillation of proof-mass

b = half width of the plate

h_0 = nominal film thickness

Pa = ambient gas pressure

4. For squeeze film damping condition, the damping coefficient (C) is given by

$$C = \frac{2\mu f(\frac{w}{l})\omega_n^3 l}{d_0^3} \qquad (2.17)$$

Where

$f(\frac{w}{l})$ = Shape function

w, l = width and length of moving plate

ω_n = Natural Frequency of the structure

d_o = Initial gap between moving and stationary plate

C = 0.05545 and

C_c (critical damping coefficient) = 2 m ω_n = 0.1033

$$\zeta = \frac{C}{C_c} = \frac{0.05545}{0.1033} = 0.54$$

Where ζ is damping factor.

As the damping factor is less than one, designed accelerometer is under-damped system. For under-damped system response time is given by

$$T(r) = \frac{1}{4\zeta\omega_n}$$

$$= 4.25\ 10^{-5}\ \text{sec}$$

2.13.2 Simulation results

To study the dynamic behavior of the accelerometer, a squeeze film damper model is made with moving proof-mass, electrodes, air gap and air column as shown in fig 2.16. The air is assumed to be moving in and out of the gaps at the four side edges of the proof-mass.

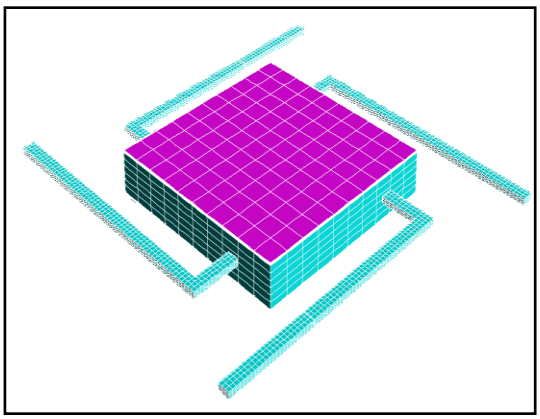

Fig. 2.16 Squeeze film damping model

2.13.3 Squeeze film damping coefficient variation with frequency

To realize a sensor with required linearity over the operational frequency range, the damping forces shall be linear within the operational frequency range and the spring force shall be low and damping coefficient shall be constant. Fig 2.17 shows the variation of damping force and spring force over large frequency range. At low frequencies, air can escape with little resistance and the spring force is small. At high frequencies, the air is held captive by its own inertia, there is not enough time for the air to move out of the way as the structure oscillates. The air gets compressed, resulting in an increased spring force. The damping is caused by viscous forces and proportional to the velocity of the oscillating structure. But, if the gas is compressed and does not move much, then the damping force will be lower. This explains why the damping gets smaller as the frequency increases above about 1 MHz.

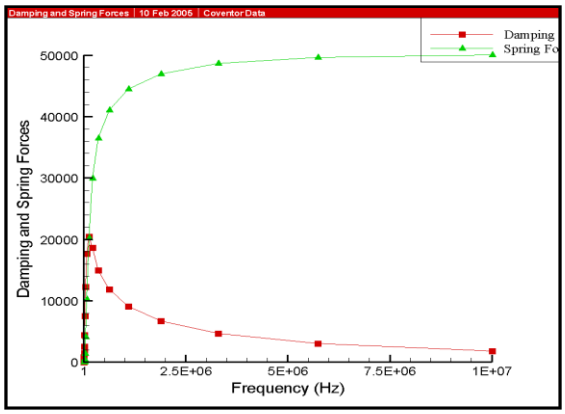

Fig 2.17 Damping analysis results over large frequency range

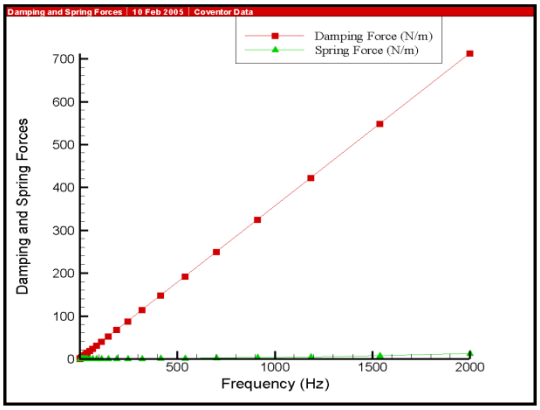

Fig 2.18 Damping analysis results over small frequency range

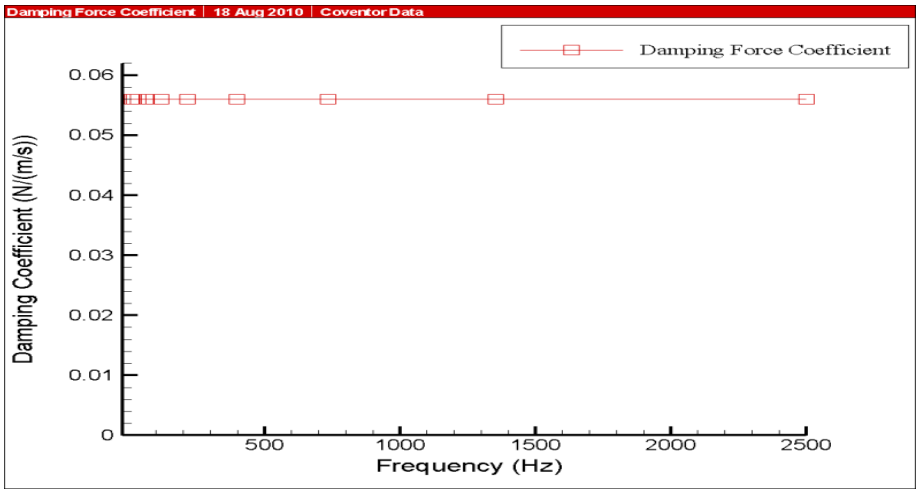

Fig.2.19 Damping coefficient variation with frequency

However, as shown in fig 2.18, within the operational frequency range of accelerometer damping force is proportional to the frequency of operation and spring force is negligible. It can be seen from fig 2.19, within the operational range of frequency damping co-efficient variation is negligible.

2.13.4 Harmonic analysis

Harmonic analysis is performed using MEMMECH module of the coventorware software to find the linearity of the accelerometer response over the required bandwidth of operation under applied acceleration. The accelerometer is subjected to a harmonic load of 30'g' at frequency ranging from 1 Hz to 100Hz. The modal-damping coefficient for the analysis is 0.055.

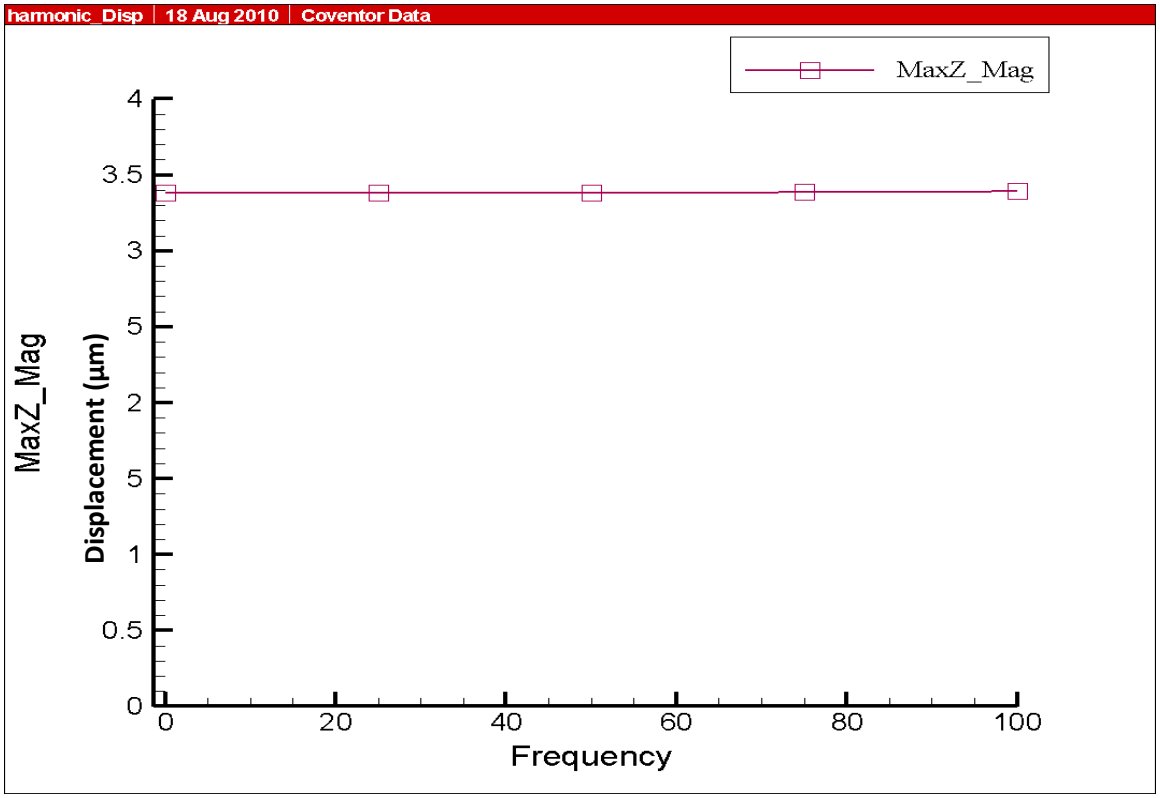

Fig.2.20. Harmonic analysis result

Fig 2.20 gives the displacement response of accelerometer at 30'g' input up to required bandwidth frequency of 100 Hz. The frequency sensitivity of displacement within the operation bandwidth is negligible.

2.14 Interface electronics

The MEMS Accelerometer is electrically equivalent to a differential parallel plate capacitor structure with the capacitance change occurring due to the change in the gap between the parallel plates. The switched-capacitor charge integration method has been widely used in MEMS capacitive sensor interface circuits [30-38]. The interface circuit shall have the following features

- Interface with the sensor with given nominal capacitance of 2.5pF and also nullify any capacitance offset that is present.
- The required output swing of the circuit is 0 to 5V with a DC bias output voltage at 0'g'
- The circuit should be able to handle a total capacitance change of 0.6pF
- The circuit should be able to resolve a minimum capacitance change of 1fF
- The bandwidth should be more than 100Hz

2.14.1 Capacitance to voltage conversion scheme

The interface circuit for converting the variation in capacitance into voltage is implemented using a standard capacitance to voltage conversion ASIC, MS3110 from Irvine Sensors.

MS3110 [39] is a general purpose, ultra noise CMOS IC that requires only a single +5V DC supply and some decoupling components. The ASIC is capable of sensing capacitance changes down to 4aF/rtHz. It can interface with either a differential capacitor pair or a single capacitive sensor.

The salient features of the IC that enables its suitability for integration with the accelerometer chips are listed below:

- Capacitance resolution: 4aF/rtHz
- Differential variable capacitance sensor interfacing
- Gain and DC offset trim
- Programmable bandwidth adjustment
- On chip EEPROM for storage of program coefficients

The ASIC functional block diagram is shown in fig 2.21.

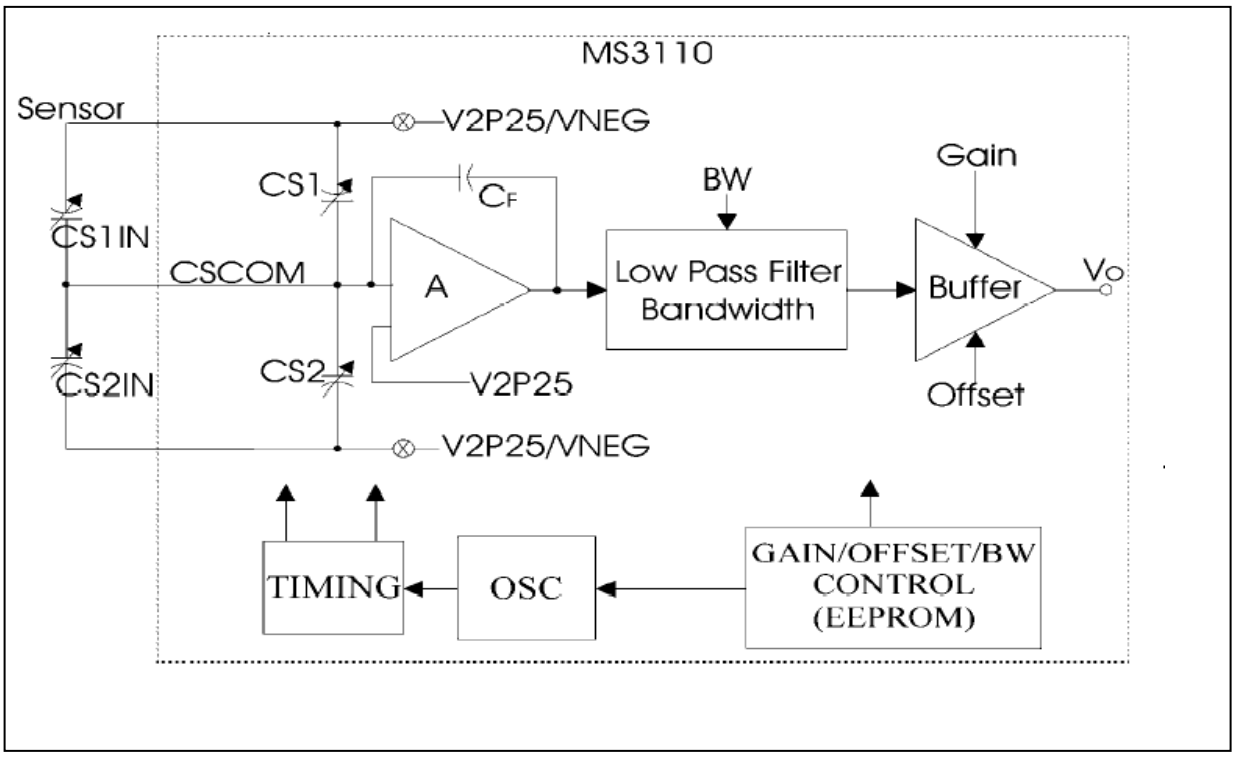

Fig 2.21 Block diagram of MS3110 ASIC

- The fundamental operation of the conversion scheme is, that of charge amplification by the trans-conductance operational amplifier interfacing the sensor capacitance bridge. The sense nodes of the capacitance bridge are fed by a square wave signal generated internally and whose amplitude oscillates between zero 'g' bias voltage and 0V.
- The amplified signal is then low pass filtered in the next section. The bandwidth of the LPF is programmable.

- The last block is a gain amplifier with the provision of gain and offset programmability. The various coefficients for capacitance bridge balancing, bandwidth, sensitivity, gain and offset are stored in an EEPROM.
- The various timing signals for EEPROM read, write, and square wave are generated internally.

The ASIC senses the change in capacitance between two capacitors and provides a voltage output proportional to the change. The transfer function of the ASIC is given as:

$$Vout = GAIN * V2P25 * 1.14 * (CS2_T - CS1_T)/CF + VREF$$

Where Vout is the output voltage

Gain = 2 or 4V/V

V2P25 = 2.25 VDC

$CS2_T$ = CS2IN + CS2

$CS1_T$ = CS1IN + CS1

CF is selected to obtain the required sensitivity

VREF can be set to 0.5V or 2.25V DC for $\Delta CS = CS2_T - CS1_T = 0$

The pin diagram of the ASIC and pin description are given in Fig 2.22 and Table 2.4 respectively.

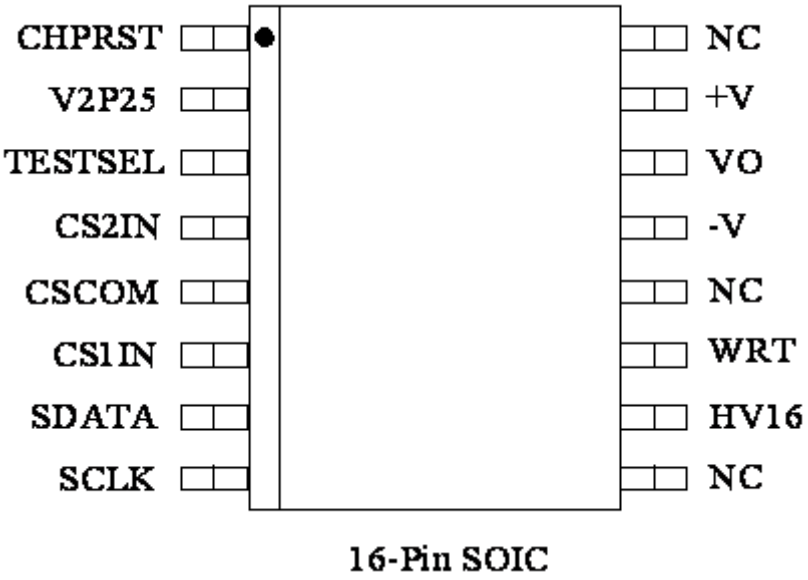

Fig 2.22 MS3110 ASIC pin diagram

Pin No	**Name**	***Description***
1	CHPRST	IC reset. Internally pulled up.
2	V2P25	2.25VDC reference
3	TESTSEL	Enables the user to bypass on-chip EEPROM and program the IC directly
4	CS2IN	Capacitor sense input 2
5	CSCOM	Capacitor sense common
6	CS1IN	Capacitor sense input 1
7	SDATA	Serial Data input, used for serial data input port for programming the EEPROM or the IC

		registers directly.
8	SCLK	Serial clock input
9	NC	No Connection
10	HV16	16VDC input port, tied to 16V when writing to EEPROM, grounded otherwise
11	WRT	Write select
12	NC	No connection
13	-V	Negative voltage rail, usually 0V
14	VO	IC Voltage output
15	+V	Positive voltage rail, usually 5V
16	NC	No connection

Table 2.4 MS 3110 pin diagram description

2.14.2 Features of the interface electronics

- The circuit gives a DC bias of 2.25V at 0'g', which is also equal to the reference voltage of the ASIC
- The sensitivity of the sensor can be programmed from 20mV/g to 66mV/g.
- Thus the maximum output swing is 2V for ±30'g'
- The fabricated accelerometer chips show a deviation in nominal capacitance values from the designed values.

- The differential capacitance bridge is not balanced at zero 'g'. As a result there is an initial offset in the output voltage when at zero 'g'. The offset is nullified by using the internal capacitances in the ASIC. In cases where the offset is much more than the limit of the internal capacitances, provision is made to add an external capacitor of suitable value in parallel with the lower capacitance in the bridge.

- Provision is made in the interface circuit board to make possible the tuning of the ASIC coefficients after the final assembly of the components on the PCB Board to cater for packaging effects also.

2.15 Results & discussion

- An accelerometer with a range of ± 30 'g' and with linearity & cross-axis sensitivity less than 1% of full scale output (FSO) is configured.
- Detailed mechanical and electrical design is done using FEA simulation techniques and the results show that the design meets required specifications of the sensor.
- Comparison of analytical and simulation results are presented in table 2.5.

Results	Analytical	FEM simulation	System level simulation
Proof-mass displacement (μm/g)	0.083	0.116	0.121
Stress at 30 'g' (MPa)	13.4	11	--
Natural frequency(Hz)	1728	1470	1432.5
Sensitivity (fF/g)	19.0	26.0	28.07
Response time (msec)	0.042	-	0.2

Table 2.5 Comparison of results

- From the comparison of results presented above it can be seen that the analytically estimated maximum displacement of the proof-mass is almost 30% less than the simulated FEM results under the applied 1 'g' acceleration.
- This is due to the fact that during analytical calculations it is estimated that the L-beams are fixed on one side and guided on the other side. However, the smaller length (l_3) of the L- beam (640microns) which is 20% of larger length (l_2) contributes to twisting in addition to bending, hence the discrepancy.